Kinetics of Rat Skin Optical Clearing at Topical Application of 40%Glucose: *Ex Vivo* and *In Vivo* Studies

Daria K. Tuchina, Polina A. Timoshina, Valery V. Tuchin, Alexey N. Bashkatov, and Elina A. Genina

***Abstract*—Optical, molecule diffusion, and mechanical properties of skin and blood microcirculation in the underlying tissues at topical application of 40%-glucose solution in rats were investigated. Optical clearing of *ex vivo* and *in vivo* skin was measured within the wavelength range of 400–900 nm using standard spectrometer, and blood microcirculation alterations was measured with laser speckle contrast imaging. Increase of skin collimated transmittance, transverse, and along skin shrinkage and weight loss was observed for the first 20–60 min of immersion, for the longer time, tissue swelling was found. The glucose diffusion coefficients in *ex vivo* and *in vivo* rat skin were evaluated as $(1.11 \pm 0.78) \times 10^{-6}$ and $(1.54 \pm 0.28) \times 10^{-6}$ cm^2/s, respectively. The decrease of average rate of microcirculation in 2.2 fold was observed. The results received allow one to evaluate glucose impact on skin tissue optical and mechanical properties and blood microcirculation.**

***Index Terms*—Optical clearing, collimated transmittance, diffuse reflectance, laser speckle contrast imaging, glucose, skin, shrinkage, swelling, glucose diffusion coefficient, blood microcirculation.**

I. Introduction

IMMERSION optical clearing is one of the innovative biomedical optics technologies that help to solve the problem of a high light scattering in tissues, which limits application of optical methods in biomedical diagnostics and therapy caused by low penetration depth of light beams and image blurring [1], [2]. Many optical clearing agents (OCAs), which are hyperosmotic, have a higher refractive index compared to tissue interstitial fluid (ISF), and may interact with hydration shell of proteins (i.e., collagen fibers which are scatterers). Thus, interaction of an OCA with a tissue induces its dehydration, reduces effective size of scatterers, and provides partial replacement of ISF by the OCA. As a result, matching of refractive indices of tissue components and their packing leads to decrease of light scattering.

'Immersion optical clearing' technique also can be used for determination of tissue permeability for exogenous or endogenous (metabolic) chemical agents [1]–[4]. Glucose-water solutions are widely used as OCAs for skin optical clearing. A number of studies with animal and human skin have shown a high optical clearing potential of glucose solutions [3]–[7]. However, comprehensive research of 40%-glucose solution impact on optical and mechanical properties of rat skin and blood microcirculation has not been made; and glucose diffusion coefficients in rat skin *ex vivo* and *in vivo* has not been evaluated. Aqueous 40%-glucose solution is biocompatible at topical application, it is hyperosmotic and has a higher refractive index ($n_{gl} = 1.391$) compared with the interstitial fluid ($n_{ISF} = 1.35$) at $\lambda = 589$ nm [8].

Temporal optical clearing of a tissue is related to rate of diffusion of glucose into tissue and induced outer water flux. In the case of similar water content in tissue and OCA solution, water flux should be minimal and molecular diffusion process can be related to glucose molecules only. Since measured diffusion coefficient can be presented as an average rate of two fluxes and water molecules diffuse much faster than glucose, the slowdown of diffusion process can indicate a strong glucose flux on the background of a weak water flux [9].

Skin contains free, bulk and protein-bound water [10]–[15]. Bulk water is a substance, where molecules are bound to each other forming a tetrahedron structure [10]–[12]. Water content in human *stratum corneum* was measured as approximately 33% (mass-%) on the surface with gradual increase to approximately 65% in deeper layers of living epidermis and dermis [16]. The total water content in rat skin was found as 54% [13] or 64.5 ± 0.7% [17] and in mouse skin as about 70% [14]. Thus, aqueous 40%-glucose solution has close water content as skin has, that leads to a preferable glucose diffusion flux in the system – skin-glucose solution [9].

Apart from the fact that glucose solution decreases light scattering in skin tissues, penetration of glucose through skin may affect cutaneous and subcutaneous blood microcirculation

Manuscript received April 8, 2018; accepted April 21, 2018. Date of publication April 26, 2018; date of current version June 12, 2018. The work (the study of the skin optical clearing and geometry of skin ex vivo) of D. K. Tuchina was supported in part by the RFBR under Grant 18-32-00587 and in part by the Scholarships of the President of the RF for young scientists. The work (impact of glucose solution on blood flow) of P. A. Timoshina was supported by the RF Ministry of Education and Science under Grant 3.1586.2017/4.6. The work (Solution of the inverse problem) of V. V. Tuchin and A. N. Bashkatov was supported by the RF Government under Grant 14.Z50.31.0044. The work (work related to the skin optical clearing in vivo) of E. A. Genina was supported by the RSF under Grant 17-73-20172. *(Alexey N. Bashkatov and Elina A. Genina contributed equally to this work.) (Corresponding author: Elina A. Genina.)*

D. K. Tuchina, P. A. Timoshina, A. N. Bashkatov, and E. A. Genina are with the Saratov State University, Saratov 410012, Russia, and also with the Tomsk State University, Tomsk 634050, Russia (e-mail: tuchinadk@mail.ru; timoshina2906@mail.ru; a.n.bashkatov@mail.ru; eagenina@yandex.ru).

V. V. Tuchin is with the Saratov State University, Saratov 410012, Russia, with the Institute of Precise Mechanics and Control, Russian Academy of Sciences, Saratov 410028, Russia, and also with the Tomsk State University, Tomsk 634050, Russia (e-mail: Tuchinvv@mail.ru).

Color versions of one or more of the figures in this paper are available online at http://ieeexplore.ieee.org.

Digital Object Identifier 10.1109/JSTQE.2018.2830500

caused by hyperosmotic properties of glucose [6]. As endothelial cells are metabolically active providing the maintenance of vascular homeostasis under physiological conditions [18], [19], it is expected that glucose may influence blood flow conditions via vascular endothelium. Such external disturbances can cause endothelial reversible dysfunction characterized by reduced endothelium-mediated vasorelaxation, hemodynamic deregulation, enhanced turnover, excessive generation of reactive oxygen species, increased oxidative stress, and enhanced permeability of the cell layer [20]. In this connection, it is important to understand how an OCA affects blood microcirculation.

Currently, one of the prospective methods for the assessment of blood flow in a full-field is the Laser Speckle Contrast Imaging (LSCI) [8], [21]–[23]. The LSCI as a noninvasive, contactless technique allowing for imaging of capillary blood flow in real-time without scanning can be effectively used to quantify OCA impact on circulation.

The goal of this study is to investigate 40%-glucose solution impact on skin optical properties and morphology, tissue dehydration and volumetric shrinkage, and on this basis to quantify glucose diffusion coefficient in rat skin *ex vivo* and *in vivo*, and to evaluate accompanied effects on skin blood microcirculation in rats *in vivo*.

II. Materials and Methods

A. Protocol of Collimated Transmittance Measurement of Skin Ex Vivo

White laboratory rats weighing 200–300 g were used in the study. The investigation of optical clearing of skin was performed on rat skin samples obtained *ex vivo* by autopsy. The area of the samples was about $10 \times 15\,\text{mm}^2$. Hairs were removed from samples with a depilatory cream before measurements. The thickness of each sample was measured before and after application of glucose solution by micrometer with a precision of 50 μm and data was averaged.

Aqueous 40%-glucose solution ("Novosibchempharm", Russia) was used as optical clearing agent. Refractive index of the 40%-glucose solution was measured using Abbe refractometer at 589 nm as $n_{gl} = 1.391$. The pH of this ready to use pharmaceutical solution was measured using pH-meter (Hanna, Germany) as 3.5.

Ten samples were used to measure collimated transmittance kinetics of skin during the optical clearing and to measure glucose diffusion coefficient in skin *ex vivo*. Intact samples were placed in cuvette with the 40%-glucose solution, and collimated transmittance spectra were measured using USB4000-Vis-NIR spectrometer (Ocean Optics, USA) in the spectral range 400–900 nm every 2−10 min during 120 min. The spectrometer was equipped with optical fibers (QP400-1-VIS-NIR, Ocean Optics, USA) with 400 μm core diameter and collimators 74-ACR (Ocean Optics, USA). Halogen lamp (HL-2000, Ocean Optics, USA) was used as a light source. Sample was fixed on the plastic plate with a central aperture and immersed in the OCA. The cuvette with a sample was placed between two optical fibers with collimators to collect the transmitted light. The scheme of the experimental setup is presented in Fig. 1. The measurements were performed at room temperature about 20 °C.

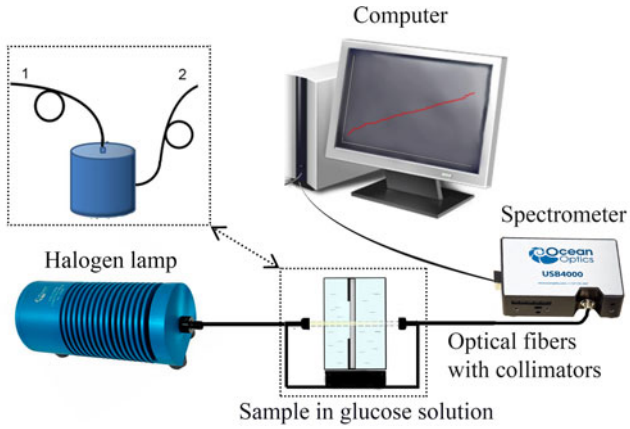

Fig. 1. The scheme of the experimental setup for *ex vivo* measurement of collimated transmittance spectra of skin samples immersed in the aqueous 40%-glucose solution. In the inset it is shown the integrating sphere for *in vivo* measurement of diffuse reflectance spectra of skin after injection of the aqueous 40%-glucose solution. 1 is the irradiating fiber, 2 is the collecting fiber.

Glucose diffusion coefficient was estimated in framework of free-diffusion model by minimization of the target function, which includes calculated ($T_{\text{c}}(D,\, t_{\text{i}})$) and experimental ($T_{\text{c}}^{*}(t_{\text{i}})$) values of the time- dependent collimated transmittance [24], using the Levenberg-Marquardt nonlinear least-squares-fitting algorithm [25]:

$$f\,(D) = \sum_{i=1}^{N_t} \left(T_c\,(D, t_i) - T_c^{*}\,(t_i)\right)^2, \tag{1}$$

where D is the diffusion coefficient, cm^2/sec; t is the time of diffusion, sec; N_t is the sampling number at registration of the temporal dependence of collimated transmittance [24].

Since glucose diffusion into the skin tissue leads to matching of refractive indices of tissue scatterers (collagen and elastin fibers) and interstitial fluid (ISF), the change of ISF amount and index of refraction was taken into account. The measured kinetics of sample weight, thickness and area was used in algorithm of estimation of glucose diffusion coefficient via change of scatterers packing. The algorithm is described in detail in Ref. [4].

Collimated transmittance data were used for estimation of the degree (efficiency) of optical clearing of skin samples. Scattering coefficient values $\mu_{\text{s}}(t)$ were obtained from transmittance data by Beer-Lambert-Bouguer law considering that in skin average absorption coefficient $\mu_{\text{a}}(t)$ is considerably smaller than scattering coefficient in this spectral range [6]:

$$T_c\,(t) = \exp\left[-\mu_t\,(t)\, l\,(t)\right]. \tag{2}$$

where $\mu_{\text{t}}(t) = \mu_{\text{a}}(t) + \mu_{\text{s}}(t)$ is the attenuation coefficient, $l(t)$ is the thickness of sample.

Degree of optical clearing of samples was evaluated as the ratio of the difference between the initial μ_{t0} and the minimally achieved μ_{tmin} values to the initial attenuation coefficient value

for different wavelengths:

$$OC_{\text{eff}} = \frac{\mu_{\text{t0}} - \mu_{\text{tmin}}}{\mu_{\text{t0}}}. \tag{3}$$

B. Protocol of Weight, Thickness, Area Measurement of Skin Samples Ex Vivo

Twenty samples of rat skin *ex vivo* were used to measure the weight, area and thickness kinetics under action of 40%-glucose solution. Weight and thickness of ten samples were measured using the electronic balance (Scientech, SA210, USA) with the precision of ± 1 mg and a micrometer with a precision of ± 10 μm, respectively, before immersion and every 5 min during the immersion. Ten samples were used for analysis of digital images of the samples for estimating sample area within a period of immersion. The color hue component of the sample image was obtained by the READ_HLS_HUE function of MathCad software (Parametric Technology Corporation, USA). To reduce the differential brightness, glare and noise, the median filter was used. The pixels, which were out of the sample area, were marked as 0. To calculate the number of pixels occupied by the sample and to convert them into the square millimeters the following equation was used [4]:

$$S = \frac{F(H_s)}{\text{cols}(H_S) \cdot \text{rows}(H_S)} \cdot \frac{\text{rows}(H) \cdot z^2}{\text{cols}(H)}, \tag{4}$$

where F is the function counting the pixels occupied by the skin sample, *rows* is the number of rows, *cols* is the number of columns, H is the original digital image, H_s is the processed image of the sample, z is the width of the image.

Measured kinetics of weight, thickness, and area during action of 40%-glucose solution on the skin samples was approximated by the following empirical equation:

$$\frac{W(t)}{W(t=0)} = A \cdot \exp\left(-\frac{t}{\tau_w}\right) + B \cdot \left(1 - \exp\left(-\frac{t}{\tau_g}\right)\right) + y_0 \tag{5}$$

where t is the time, $W(t)$ and $W(t=0)$ are the values of measured parameter (weight, thickness or area) at t and $t=0$, respectively; A and B are coefficients, characterizing the maxima of dehydration/shrinkage or swelling degree, respectively; τ_{w} and τ_{g} are the characteristic diffusion time constants of water and glucose, respectively; and y_0 is the residual value of the parameter.

C. Protocol of Diffuse Reflectance Measurement of Skin In Vivo

The investigation of optical clearing impact on skin diffuse reflectance was performed *in vivo* for five rats. The animals were anaesthetized by intramuscular injection of 0.18–0.2 mL of Zoletil 50 (Vibrac, France). The hair was removed from the skin surface using a depilatory cream.

Aqueous 40%-glucose solution was injected under the skin in the back area of the animals. The volume of the injection was 0.1 mL.

Measurements of diffuse reflectance spectra of rat skin were performed in the spectral range from 400 to 800 nm using USB4000-Vis-NIR spectrometer equipped with the integrating sphere ISP-80-8-R (Ocean Optics, USA) (Fig. 1, the inset). Backscattered radiation was collected from the skin area of about 10 mm in diameter. The spectrometer was calibrated using a reflectance standard WS-1-SL (Labsphere, USA) with a smooth surface.

When detecting the reflected signal from the skin, the sphere was placed directly in the area of injection of the glucose solution on the surface of the skin. The measurements were performed first on intact skin and then every 2 min after injection during 100–120 min.

The quantification of glucose diffusion coefficient in skin was carried out using measurements of the temporal evolution of the diffuse reflectance and the approach of Ref. [24] for solution of the inverse problem by minimization of the target function:

$$F(D) = \sum_{i=1}^{N_t} \left(R\left(D, t_i\right) - R^*\left(t_i\right)\right)^2, \tag{6}$$

where $R\,(D, t)$ and $R^*(D,\ t)$ are the calculated and experimental values of the time-dependent diffuse reflectance, respectively; and N_t is the number of time points obtained at registration of the temporal kinetics of the reflectance.

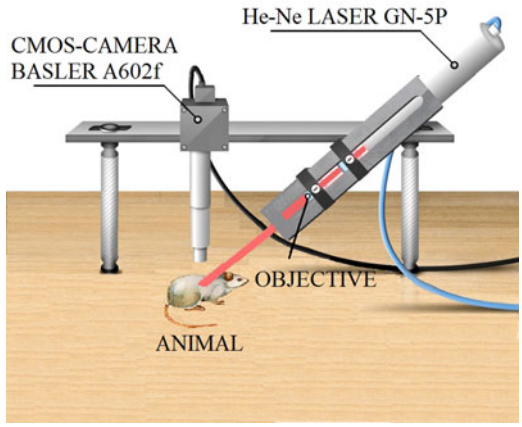

Fig. 2. The scheme of experimental setup for measurement of blood microcirculation in rat hypodermis.

D. Protocol for Monitoring of Blood Microcirculation In Vivo

The monitoring of blood microcirculation in rat hypodermis at 40%-glucose solution impact was carried out for ten experimental animals using a homemade experimental LSCI setup (Fig. 2).

He–Ne laser GN-5P (Russia) was used as a light source (wavelength 632.8 nm). The monochrome CMOS camera (Baslera802f, number of pixels in the matrix 656 $\times$ 491, pixel size 9.9 $\times$ 9.9 μm, 8 bit per pixel) with the fixed exposure time of 20 ms, combined with the LOMO objective (10$\times$, St. Petersburg, Russia) was used as a detector.

To calculate the contrast of speckle images, the following relation was used [26]:

$$V_k = \sigma_{I\,k} / \bar{I}_k, \tag{7}$$

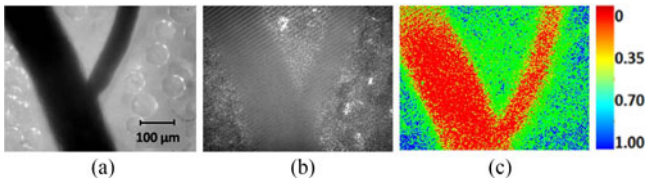

Fig. 3. The image of the vessel (diameter 280 μm) obtained by a digital microscopy (a), speckle image in coherent light (632.8 nm) (B&W) (b) and calculated distribution of laser speckle contrast (1-0) (colored). Scale corresponds to 100 μm.

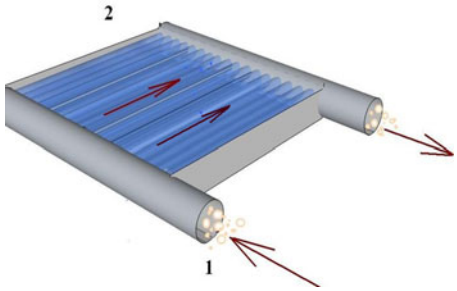

Fig. 4. Schematic representation of skin phantom: 1 is the suspension of particles (diameter ~7–9 μm); 2 is the phantom with the surface area $\sim 2 \times 2$ cm^2, number of channels (blood capillaries) of ~300 and their diameters of ~180–200 μm).

where k is the number of frames in a sequence of speckle-modulated images, $\bar{I}_k$ and $\sigma_{I\,k}$ are the scattered light intensity averaged over the analyzed frame and the root-mean-square value of the fluctuation component of the pixel's brightness, respectively:

$$\bar{I}_k = (1/MN) \sum_{m=1}^{M} \sum_{n=1}^{N} I_k\,(m,n), \tag{8}$$

$$\sigma_{I\,k} = \sqrt{(1/MN) \sum\nolimits_{m=1}^{M} \sum\nolimits_{n=1}^{N} \left\{ I_k\,(m,n) - \bar{I}_k \right\}^2}, \tag{9}$$

where M and N are the number of pixels in rows and columns of the analyzed area of the frame, respectively; $I_k(m,\ n)$ is the brightness of the (m, n) -pixel of the k-frame.

To perform the measurements and calculate the contrast, we developed a program in the LabVIEW 8.5 environment (National Instruments, USA) that allowed one to record the intensity distribution of the speckle field with the rate of 100 frames per sec in real time and calculate the mean contrast or its spatial distribution using Eq. (7) with parallel imaging in the region chosen by the operator. Speckle images were recorded during one minute, and then mean value and standard deviation of the contrast of speckle images was calculated. Fig. 3 shows the images of a typical blood vessel (a), obtained by a digital microscopy, the spatial distribution of the measured speckle local contrast (b) in coherent light, and its normalized distribution (c). The diameter of the investigated vessels varied in the range from 100 μm to 250 μm.

For quantitative evaluation of blood velocity, a preliminary calibration of the LSCI setup was carried out using a specially designed skin blood flow phantom (Fig. 4) [27]. Flow of the scattering fluid (blood model) through multiple channels (blood capillaries) of this phantom at the specified speeds was provided by using a commercial drug dispenser. The calibration relationship between contrast of the speckle images $<V>$ and the velocity (mm/sec) of the model particles was obtained (Fig. 5).

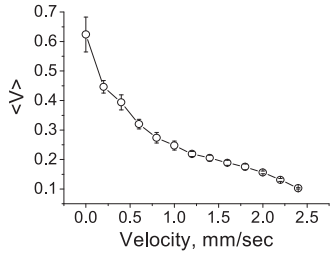

Fig. 5. Phantom studies: the experimental calibration curve: relationship between speckle contrast and velocity of particles.

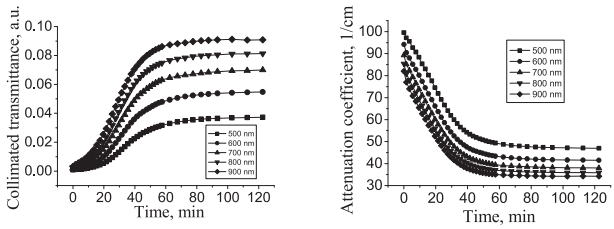

Fig. 6. Typical kinetic curves for collimated transmittance (a) and reconstructed corresponding attenuation coefficient (b) of *ex vivo* skin sample during its immersion in 40%-glucose solution measured for different wavelengths.

III. Results

The typical temporal dependence of collimated transmittance of *ex vivo* rat skin sample immersed in 40%-glucose solution measured at different wavelengths is presented in Fig. 6(a). It is seen that transmittance of intact skin sample is low. Increase of collimated transmittance observed during action of glucose solution is associated with attenuation coefficient reduction (Fig. 6(b)). Optical clearing process saturates to 60–90 min of immersion. In the studied spectral range, collimated transmittance increases with the wavelength.

Experimental data for degree (efficiency) of optical clearing of skin *ex vivo* in different wavelength ranges was evaluated by using Eq. (3) as 0.27 ± 0.12. Large standard deviation of the efficiency is in the limits of the natural spreading of optical, structural, and morphological properties of the skin from sample to sample.

Kinetics of weight, thickness and area of skin samples under the action of 40%-glucose solution normalized to their initial values, averaged by all measured samples, and approximated by Eq. (5) is presented in Fig. 7. The volume kinetics was obtained by multiplication of thickness and area.

All measured parameters decreased at the beginning of immersion. The decrease of weight (dehydration) continued about 1 hr; it took about 20 min for thickness decreasing (transverse shrinkage) and area decreasing (along shrinkage). Statistical analysis of the data using Student's t-test demonstrated that there was a significant difference between initial and minimal values of these parameters ($p < 0.05$). For the longer time, the

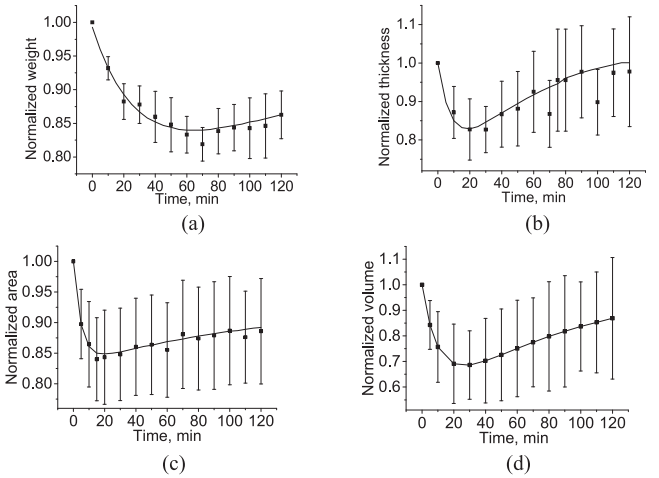

Fig. 7. The kinetics of weight (a), thickness (b), area (c), and volume (d) of *ex vivo* skin samples under the action of 40%-glucose solution approximated accordingly to Eq. (5).

TABLE I
KINETIC PARAMETERS FOR SHRINKAGE AND SWELLING OF RAT SKIN SAMPLES

	A	τ_w, min	B	τ_g, min	y_0
Weight, g	0.29±0.07	29±9	0.28±0.22	124±90	0.69±0.07
Thickness, mm	0.34±0.08	12±5	0.42±0.19	81±49	0.66±0.07
Area, mm^2	0.20±0.05	10±12	0.13±0.11	120±66	0.80±0.05
Volume, mm^3	0.44	9.8	0.52	130	0.56

± Standard deviation

subsequent slight weight increase (but not to the initial value), as well as transverse and along swelling of skin samples were observed. During 2 hrs, sample thickness, area, and volume were going back more or less to the initial state. Differences between their initial and final values were not statistically significant ($p > 0.05$).

The following kinetic parameters of dehydration/shrinkage and swelling of rat skin samples under the action of 40%-glucose solution are presented in Table I the dehydration (A) and swelling (B) coefficients, the characteristic diffusion time constants for water (τ_w) and glucose (τ_g), and the residual value of the parameter (y_0) obtained by approximation of experimental results with Eq. (5). The greater change in both shrinkage ($A = 0.34 \pm 0.08$) and swelling ($B = 0.42 \pm 0.19$) stages was observed for thickness. The change of the sample area ($A = 0.20 \pm 0.05$, $B = 0.13 \pm 0.11$) was less expressed. Weight decreasing took more time ($\tau_w = 29 \pm 9$ min) than for both types of shrinkage. Volume kinetics combined two processes—transverse and along change of sample geometry, that was why it had the highest values of swelling degree ($B = 0.52$) and the maximum of shrinkage ($A = 0.44$).

The measured kinetics of skin collimated transmittance and the skin shrinkage/swelling parameters was used for estimation of glucose diffusion coefficient to take into account the tissue shrinkage/swelling and weight variation in the course of

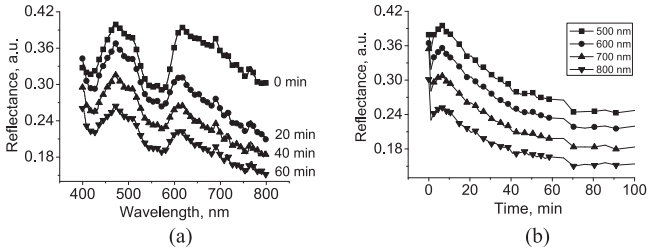

Fig. 8. Diffuse reflectance spectra (a) and corresponding kinetics (b) of rat skin *in vivo* after subcutaneous injection of 40%-glucose solution.

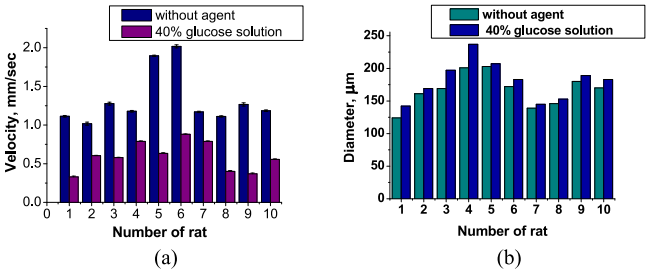

Fig. 9. Variation of velocity of blood (a) and diameter of blood vessels (b) in hypodermis of rats *in vivo* without and with 40%-glucose action.

optical clearing. The glucose diffusion coefficient averaged by all samples was estimated as $(1.11 \pm 0.78) \times 10^{-6}$ cm^2/sec.

The typical spectra and kinetics of rat skin diffuse reflectance *in vivo* after topical injection of 40%-glucose solution measured in the area near injection site are presented in Fig. 8. The first spectrum corresponds to the spectrum of native skin. After the glucose injection, the decrease of skin reflectance is observed in a whole spectral range (Fig. 8(a)) that corresponds to the decrease of skin scattering.

However, we can see in Fig. 8(b) the immediate drop and then 8–9 min-long slight increase of diffuse reflectance just after injection. It can be connected with some transition phenomena happened immediately after injection and volumetric redistribution of glucose and induced local water flux, as well as with physiological reaction of skin on glucose injection. In particular, a white (scattering) ring aroused around skin puncture by injecting needle on some distance from the central area that affected by the glucose solution (where optical clearing is seen) on the border with untreated native skin, similarly as it was described in Ref. [6]. This ring corresponded to edema caused by water inflow from surrounding to the place of injection. Then the diffusion of glucose to surrounding tissue led to the matching of refractive indices of tissue components and thus, to the decrease of the scattering. It manifested in diffuse reflectance further decrease. The decrease during 70-80 min in relation to the diffuse reflectance of the intact skin was 1.5-1.8 fold in dependence on the wavelength.

Diffusion coefficient of glucose in *in vivo* rat skin was evaluated as $(1.54 \pm 0.28) \times 10^{-6}$ cm^2/sec.

Data received from measurements of 40%-glucose solution impact on blood microcirculation and diameter of blood vessels in rats *in vivo* with LSCI are shown in Fig. 9. The histograms present values of blood velocity (Fig. 9(a)) and diameter of blood

vessels (Fig. 9(b)) before and after application of 40%-glucose solution for each animal.

The averaged values and standard deviations of blood velocity for ten laboratory rats before and after glucose impact were 1.32 $\pm$ 0.34 mm/sec and 0.59 $\pm$ 0.19 mm/sec, respectively. There was a statistically significant difference between these values ($p < 0.001$). The averaged values and standard deviations of vessels diameter before and after glucose impact were 166 $\pm$ 25 μm and 180 $\pm$ 16 μm, respectively. There was no a significant difference between these parameters ($p > 0.05$). The results have shown that applying of 40%-glucose solution has led to reduction of blood flow velocity (about 2.2 fold) at the insignificant vasodilatation (about 8%).

IV. Discussion

Optical clearing of tissues can be monitored by measuring tissue optical transmittance [2], [4], [5], [9] or diffuse reflectance [1], [2], [5]–[7], [28] during action of applied OCA. We have observed increase of skin collimated transmittance in *ex vivo* measurements and reduction of skin diffuse reflectance in *in vivo* measurements. Attenuation of the light beam decreases because of reduction of skin scattering [1].

Refractive index matching and dehydration induced by osmotic properties of glucose are essential for optical clearing of skin [1]–[3], [28]. These two mechanisms play main role in scattering decrease. Collagen dissociation [3], [5] does not make a significant contribution because of short time of glucose action.

The efficiency of optical clearing of *ex vivo* skin in the wavelength range 500–900 nm was about 0.27 $\pm$ 0.12. Result of evaluation of efficiency of mice skin optical clearing *ex vivo* under action of 43% glucose solution, provided in Ref. [4], is 0.52 $\pm$ 0.9. Significant difference between results obtained in this experiments and in Ref. [4] may be connected with different pH of the used solutions ($pH_{gl40\%} = 3.5$ and $pH_{gl43\%} = 5.7$), since refractive indices of both solutions are very close. Tissue swelling apparently decreases the total transparency of skin.

Decrease of weight (water lost) is resulted by outflow of free water contained in ISF from the sample induced by hyperosmotic action of glucose. In Refs. [4], [29]–[31] it has been shown the tissue water loss under action of glycerol and glucose solutions. Water loss causes the transverse and along shrinkage, which are connected with the rearrangement of fiber packing in the sample during immersion in glucose solution [4]. Since the decrease of the distance between skin fibers is much more likely than the change of fiber length, more strong transverse shrinkage compared to along shrinkage is observed. Skin swelling is a result of the change of ISF pH ($pH_{ISF} = 7.4$ [32]) due to impact of glucose solution with lower pH ($pH_{gl} = 3.5$). As it has been shown in Ref. [33], skin samples under action of polyethylene glycols with $pH = 6.5$ have not swelled during 120 min.

Diffuse reflectance spectra allow one to conclude about impact of glucose on skin microvessels during optical clearing. In Ref. [28], it has been shown deformation of skin reflectance spectra in the range corresponding to the blood absorption in 10 min after subcutaneous injection of glycerol solution with high concentration (84.4%). The deformation is related to the transition of hemoglobin from the oxygenated form to the deoxygenated one [34] caused by hemostasis in microvessels and capillaries in dermis [28]. Under action of 40%-glucose solution, the spectral transformation in hemoglobin absorption range is not observed that indicates the absence of hemostasis. It is confirmed by earlier performed experiments with human skin clearing using 40%-glucose solution [7].

Direct investigation of blood vessels using LSCI has shown that application of 40%-glucose solution provides small blood vessels expansion by 8% and corresponding blood flow decreasing in 2.2 fold. It correlates with the data presented in Refs. [6] and [35] at topical application of glucose solution on rat mesentery and chick chorioallantoic membrane. The use of osmotic glucose solution causes endothelial dysfunction and permeability changes; the solution attracts water from the surrounding tissues, thereby increasing the diameter of the vessels and accordingly slowing down blood flow.

Calculations of glucose diffusion coefficients in rat skin on the basis of *ex vivo* and *in vivo* measurements have been performed for 10 wavelengths, and the obtained values have been averaged. There are $(1.11 \pm 0.78) \times 10^{-6}$ and $(1.54 \pm 0.28) \times 10^{-6}$ cm^2/ sec, respectively.

It is seen that the value of diffusion coefficient estimated from *in vivo* measurements is larger than that from *ex vivo* measurements. This can be explained by the influence of temperature dependence of diffusion coefficient and involvement of physiology in glucose diffusion in living tissues.

It is well known that diffusion coefficient is increased with the increase of temperature of the solution. The temperature dependence can be expressed as follows [36]:

$$D_{\mathrm{Corr}} = D_{\mathrm{Exvivo}} \times \frac{T_{37^\circ\mathrm{C}}}{T_{20^\circ\mathrm{C}}} \times \frac{\eta_{20^\circ\mathrm{C}}}{\eta_{37^\circ\mathrm{C}}}, \tag{10}$$

where D_{Corr} is the diffusion coefficient corrected on physiological temperature 37°C, $D_{\mathrm{Ex\,vivo}}$ is the diffusion coefficient estimated from *ex vivo* measurements, $T_{37^\circ\mathrm{C}}$ and $T_{20^\circ\mathrm{C}}$ are the temperature of skin (in °K), $\eta_{20^\circ\mathrm{C}}$ and $\eta_{37^\circ\mathrm{C}}$ are the viscosity of glucose solution at different temperatures. The values of viscosity were obtained from Ref. [37] as $\eta_{20^\circ\mathrm{C}} = 3.02$ mPa·sec and $\eta_{37^\circ\mathrm{C}} = 1.92$ mPa·sec. Extrapolating the obtained value of the diffusion coefficient to the physiological temperature, we have found that the mean value of glucose diffusion coefficient in skin at 37 °C is $(1.85 \pm 1.3) \times 10^{-6}$ cm^2/sec. It is seen that the obtained value is larger than the value of glucose diffusion coefficient estimated from *in vivo* measurements. It can be explained by different geometry of *in vivo* and *ex vivo* measurements. At *ex vivo* measurements the volume of glucose exceeds significantly the volume of the skin sample. In contrast, at *in vivo* experiment the volume of injected solution is limited but surrounding tissue can be considered as unlimited. Thus, influence of organism hinders manifestation of optical clearing due to permanent water inflowing from surrounding tissue into the probing volume.

Some slow-down of glucose diffusion rate in living tissues can be due to its metabolic uptake by the surrounding cells in the course of diffusion [38].

Recently, the diffusion coefficient of 43%-glucose solution in mice skin has been estimated *ex vivo* as $(2.70 \pm 2.22) \times$

10^{-6} cm^2/sec [4]. The value of the diffusion coefficient measured in this paper [$(1.11 \pm 0.78) \times 10^{-6}$ cm^2/sec] is somewhat smaller than the value obtained in Ref. [4]. In our opinion, the difference in the values of the diffusion coefficients is due to the difference in the water content in these tissues. So for the mouse skin, the water content is about 70% [14], while for the rat skin the water content is 54% [13] or 64.5 $\pm$ 0.7% [17]. Obviously, the diffusion rate will be greater for a tissue with the higher water content.

In Ref. [7], the diffusion coefficient of 40% glucose solution in human skin *in vivo* was presented. It was estimated as $(2.56 \pm 0.13) \times 10^{-6}$ cm^2/sec and characteristic time of diffusion τ (time of decrease of reflectance in *e* fold) was 19.3 $\pm$ 4.6 min. Value of τ estimated from kinetics of *in vivo* rat skin reflectance in this paper is 19.8 $\pm$ 5.0 min. Thus, diffusion time in the both experiments is approximately equal. Apparently, differences in the values of diffusion coefficients also can be explained by differences in water content in human and rat skin. In Ref. [17], it was shown that water content in human skin falls to the range from 68.5% to 73.4% vs 54–64% for rat skin. It is obvious that differences in the tortuosity of the diffusion paths for these types of skin, due to differences in their structural and morphological properties, also contribute to the difference in diffusion coefficient values.

V. Conclusion

The increase of collimated transmittance of *ex vivo* rat skin during action of 40%-glucose solution was obtained. Efficiency of optical clearing of *ex vivo* skin in the wavelength range 400–900 nm was evaluated as 0.27 $\pm$ 0.12. Weight loss and transverse and along shrinkage of skin immersed in glucose solution at the beginning of optical clearing process; and subsequent recovery of the parameters were observed. Sharp decrease in the skin diffuse reflectance parameter *in vivo* just after subcutaneous injection, then increasing during 8–9-min, and then about one hour gradual decrease in 1.5–1.8 folds was registered. The glucose diffusion coefficient in *ex vivo* and *in vivo* skin was estimated basing on the results of these measurements as $(1.11 \pm 0.78) \times 10^{-6}$ and $(1.54 \pm 0.28) \times 10^{-6}$ cm^2/sec, respectively. It was demonstrated a low vasodilator effect, expressed in the decrease of average rate of microcirculation in 2.2 fold. However, deoxygenation of blood hemoglobin due to hemostasis did not occur.

The obtained results have shown that 40%-glucose solution is prospective agent for the use in optical diagnostics. Although the efficiency of optical clearing of 40%-glucose solution is lower than that of, for example, PEGs and glycerol [30], [33] however impact of glucose provides a more sparing mode of optical clearing. High dehydration of such hyperosmotic agents as glycerol can induce damage of blood vessels and necrosis of tissues at the subcutaneous injection as was shown in Refs [6], [28]. The 40%-glucose solution has shown low dehydration impact on skin and insignificant vasodilatation that can allow one to use it on human skin *in vivo*.

The obtained results can be used for optimization of tissue optical clearing and drug delivery techniques, improvement of biophysical and mathematical models describing interactions between tissues and optical clearing agents.

Acknowledgment

The authors would like to thank Dr. V. Lychagov for designing skin blood flow phantom and Dr. A. B. Bucharskaya for providing laboratory animals.

References

[1] V. V. Tuchin, "A clear vision for laser diagnostics," *IEEE J. Sel. Topics Quantum Electron.*, vol. 13, no. 6, pp. 1621–1628, Nov./Dec. 2007.
[2] E. A. Genina, A. N. Bashkatov, Yu. P. Sinichkin, I. Yu. Yanina, and V. V. Tuchin, "Optical clearing of biological tissues: Prospects of application in medical diagnostics and phototherapy [Review]," *J. Biomed. Photon. Eng.*, vol. 1, no. 1, pp. 22–58, 2015.
[3] J. Wang *et al.*, "Sugar-induced skin optical clearing: From molecular dynamics simulation to experimental demonstration," *IEEE J. Sel. Topics Quantum Electron.*, vol. 20, no. 2, Mar./Apr. 2014, Art. no. 7101007.
[4] D. K. Tuchina *et al.*, "*Ex vivo* optical measurements of glucose diffusion kinetics in native and diabetic mouse skin," *J. Biophoton.*, vol. 8, no. 4, pp. 332–346, 2015.
[5] J. Hirshburg, B. Choi, J. S. Nelson, and A. T. Yeh, "Correlation between collagen solubility and skin optical clearing using sugars," *Laser Surg. Med.*, vol. 39, no. 2, pp. 140–144, 2007.
[6] E. I. Galanzha *et al.*, "Skin backreflectance and microvascular system functioning at the action of osmotic agents," *J. Phys. D, Appl. Phys.*, vol. 36, no. 14, pp. 1739–1746, 2003.
[7] V. V. Tuchin, A. N. Bashkatov, E. A. Genina, Yu. P. Sinichkin, and N. A. Lakodina, "*In vivo* investigation of the immersion-liquid-induced human skin clearing dynamics," *Tech. Phys. Lett.*, vol. 27, no. 6, p. 489–490, 2001.
[8] V. V. Tuchin, *Tissue Optics: Light Scattering Methods and Instruments for Medical Diagnostics*, 3rd ed. Bellingham, WA, USA: SPIE, 2015.
[9] L. M. Oliveira, M. I. Carvalho, E. Nogueira, and V. V. Tuchin, "The characteristic time of glucose diffusion measured for muscle tissue at optical clearing," *Laser Phys.*, vol. 23, no. 7, 2013, Art. no. 075606.
[10] S. H. Chung, A. E. Cerussi, S. I. Merritt, J. Ruth, and B. J. Tromberg, "Non-invasive tissue temperature measurements based on quantitative diffuse optical spectroscopy (DOS) of water," *Phys. Med. Biol.*, vol. 55, no. 13, pp. 3753–3765, 2010.
[11] K. A. Martin, "Direct measurement of moisture in skin by NIR spectroscopy," *J. Soc. Cosmetic Chem.*, vol. 44, pp. 249–261, 1993.
[12] A. Roggan, M. Friebel, K. Dörschel, A. Hahn, and G. Müller, "Optical properties of circulating human blood in the wavelength range 400-2500 nm," *J. Biomed. Opt.*, vol. 4, no. 1, pp. 36–46, 1999.
[13] P. Ballard, D. E. Leahy, and M. Rowland, "Prediction of *in vivo* tissue distribution from *in vitro* data 1. Experiments with markers of aqueous spaces," *Pharmaceutical Res.*, vol. 17, no. 6, pp. 660–663, 2000.
[14] Y.-A. Woo, J.-W. Ahn, I.-K. Chun, and H.-J. Kim, "Development of a method for the determination of human skin moisture using a portable near-infrared system," *Anal. Chem.*, vol. 73, no. 20, pp. 4964–4971, 2001.
[15] A. A. Gurjarpadhye, W. C. Vogt, Y. Liu, and C. G. Rylander, "Effect of localized mechanical indentation on skin water content evaluated using OCT," *Int. J. Biomed. Imag.*, vol. 2011, 2011, Art. no. 817250.
[16] Ch. S. Choe, J. Schleusener, J. Lademann, and M. E. Darvin, "Keratin-water-NMF interaction as a three layer model in the human stratum corneum using *in vivo* confocal Raman microscopy," *Sci. Rep.*, vol. 7, 2017, Art. no. 15900.
[17] R. F. Reinoso, B. A. Telfer, and M. Rowland, "Tissue water content in rats measured by desiccation," *J. Pharmacological Toxicological Methods*, vol. 38, no. 2, pp. 87–92, 1997.
[18] P. Vallance, "Importance of asymmetrical dimethylarginine in cardiovascular risk," *Lancet*, vol. 358, no. 9299, pp. 2096–2097, 2001.
[19] P. O. Bonetti, L. O. Lerman, and A. Lerman, "Endothelial dysfunction: A marker of atherosclerotic risk," *Arteriosclerosis Thrombosis Vascular Biol.*, vol. 23, no. 2, pp. 168–175, 2003.
[20] C. M. Sena, A. M Pereira, and R. Seiça, "Endothelial dysfunction—A major mediator of diabetic vascular disease," *Biochimica Biophys. Acta*, vol. 1832, no. 12, pp. 2216–2231, 2013.
[21] D. Briers *et al.*, "Laser speckle contrast imaging: Theoretical and practical limitations," *J. Biomed. Opt.*, vol. 18, no. 6, 2013, Art. no. 066018.

[22] R. Shi, M. Chen, V. V. Tuchin, and D. Zhu, "Accessing to arteriovenous blood flow dynamics response using combined laser speckle contrast imaging and skin optical clearing," *Biomed. Opt. Express*, vol. 6, no. 6, pp. 1977–1989, 2015.
[23] P. A. Timoshina, A. B. Bucharskaya, D. A. Alexandrov, and V. V. Tuchin, "Study of blood microcirculation of pancreas in rats with alloxan diabetes by laser speckle contrast imaging," *J. Biomed. Photon. Eng.*, vol. 3, no. 2, 2017, Art. no. 020301.
[24] A. N. Bashkatov, E. A. Genina, and V. V. Tuchin, "Measurement of glucose diffusion coefficients in human tissues," in *Handbook of Optical Sensing of Glucose in Biological Fluids and Tissues*, V. V. Tuchin, Ed. Boca Raton, FL, USA: Taylor & Francis, 2009, pp. 587–621.
[25] W. H. Press, S. A. Tuekolsky, W. T. Vettering, and B. P. Flannery, *Numerical Recipes in C: The Art of Scientific Computing*. Cambridge, U.K.: Cambridge Univ. Press, 1992.
[26] J. D. Briers, "Laser Doppler, speckle and related techniques for blood perfusion mapping and imaging," *Physiol. Meas.*, vol. 22, no. 4, pp. R35–R66, 2001.
[27] V. V. Tuchin *et al.*, "Finger tissue model and blood perfused skin tissue phantom," *Proc. SPIE*, vol. 7898, 2011, Art. no. 78980Z.
[28] E. A. Genina, A. N. Bashkatov, Yu. P. Sinichkin, and V. V. Tuchin, "Optical clearing of skin under action of glycerol: *Ex vivo* and *in vivo* investigations," *Opt. Spectrosc.*, vol. 109, no. 2, pp. 225–231, 2010.
[29] C. G. Rylander *et al.*, "Dehydration mechanism of optical clearing in tissue," *J. Biomed. Opt.*, vol. 11, no. 4, 2006, Art. no. 041117.
[30] E. A. Genina *et al.*, "Optical clearing of human skin: comparative study of permeability and dehydration of intact and photothermally perforated skin," *J. Biomed. Opt.*, vol. 13, no. 2, 2008, Art. no. 021102.
[31] T. Yu, X. Wen, V. V. Tuchin, Q. Luo, and D. Zhu, "Quantitative analysis of dehydration in porcine skin for assessing mechanism of optical clearing," *J. Biomed. Opt.*, vol. 16, no. 9, 2011, Art. no. 095002.
[32] Y. Marunaka, "Roles of interstitial fluid pH in diabetes mellitus: Glycolysis and mitochondrial function," *World J. Diabetes*, vol. 6, no. 1, pp. 125–135, 2015.
[33] D. K. Tuchina, V. D. Genin, A. N. Bashkatov, E. A. Genina, and V. V. Tuchin, "Optical clearing of skin tissue *ex vivo* with polyethylene glycol," *Opt. Spectrosc.*, vol. 120, no. 1, pp. 28–37, 2016.
[34] S. A. Prahl, 1999. [Online]. Available: https://omlc.org/spectra/hemoglobin/index.html.
[35] D. Zhu *et al.*, "Short-term and long-term effects of optical clearing agents on blood vessels in chick chorioallantoic membrane," *J. Biomed. Opt.*, vol. 13, no. 2, 2008, Art. no. 021106.
[36] I. S. Grigoriev and E. Z. Meylikhov, Eds., *Physical Values Handbook*. Moscow, Russia: EnergoAtomIzdat, 1991.
[37] A. V. Bui and M. N. Nguyen, "Prediction of viscosity of glucose and calcium chloride solutions," *J. Food Eng.*, vol. 62, pp. 345–349, 2004.
[38] R. J. Gillies, I. Robey, and R. A. Gatenby, "Causes and consequences of increased glucose metabolism of cancers," *J. Nucl. Med.*, vol. 49, no. 6, pp. 24S–42S, 2008.

Daria K. Tuchina received the Ph.D. degree in biophysics in 2016. She is an Assistant Professor and an Engineer with the Department of Optics and Biophotonics, Saratov State University, Saratov, Russia. She is the co-author of 35 publications, more than 50 reports, 2 patents, and participant of more than 20 scientific projects. Her researches are focused on tissue optical clearing, investigation of diabetic tissues, and quantification of diffusion of chemical agents in tissues. She is the secretary of the "Internet Biophotonics" section of the annual international conference Saratov Fall Meeting.

Polina A. Timoshina received the Ph.D. degree in biophysics in 2016. She is an Assistant Professor and an Engineer with the Department of Optics and Biophotonics, Saratov State University, Saratov, Russia. She is the co-author of 21 publications. Her research interests include tissue optics, laser medicine, tissue optical clearing, and speckle contrast imaging.

Valery V. Tuchin is a Professor and the Head of Optics and Biophotonics with Saratov State University, Saratov, Russia, and several other universities. His research interests include tissue optics, laser medicine, tissue optical clearing, and nanobiophotonics. He is a recipient of the Honored Science Worker of the Russia, the Honored Professor of Saratov University, the SPIE Educator Award, FiDiPro (Finland), the Chime Bell Prize of Hubei Province (China), and the Joseph W. Goodman Book Writing Award (OSA/SPIE). He has 19577 citations and h-index 65 (Google Scholar, May 7, 2018). He is a fellow of the SPIE and the OSA.

Alexey N. Bashkatov is an Associate Professor with the Departments of Optics and Biophotonics and the Head of the Laboratory of Biomedical Optics of Research-Educational Institute of Optics and Biophotonics, Saratov State University, Saratov, Russia. He is a co-author of more than 250 invited and contributed publications, 8 book chapters, and 9 patents. His research interests include study of optical properties of tissues, spectroscopy, and modeling of light propagation in turbid media. He has 2200 citations and h-index 22 (WoS, April 7, 2018).

Elina A. Genina is an Associate Professor with the Departments of Optics and Biophotonics, Saratov State University, Saratov, Russia. She is a co-author of more than 250 peer-reviewed publications, 8 book chapters, and 9 patents. Her research interests include biomedical optics, laser medicine, and development of methods for control of tissue absorption and scattering properties for medical optical diagnostics and therapy. She is a scientific secretary of the International Symposium on Optics and Biophotonics (Saratov Fall Meeting). She has 2165 citations and h-index 22 (WoS, April 7, 2018).